Electrochemistry Communications 35 (2013) 100–103

Contents lists available at ScienceDirect

Electrochemistry Communications

journal homepage: www.elsevier.com/locate/elecom

Short communication

Investigation of hydrogen evolution and enrichment by scanning Kelvin probe force microscopy

Gang Wang, Yu Yan, Xina Yang, Jinxu Li *, Lijie Qiao

Corrosion and Protection Center, Key Laboratory for Environmental Fracture (MOE), University of Science and Technology Beijing, Beijing 100083, China

ARTICLE INFO

Article history:
Received 1 July 2013
Received in revised form 1 August 2013
Accepted 5 August 2013
Available online 13 August 2013

Keywords:
Hydrogen
Surface potential
Work function
Scanning Kelvin probe force microscopy (SKPFM)
Maraging steel

ABSTRACT

It has been a challenge to detect the real-time distribution of hydrogen at the micro-level. In this study, a scanning Kelvin probe force microscopy (SKPFM) was employed to characterize the surface potential changes induced by hydrogen. Variations of the surface potential were used to assess (a) the real-time distribution of hydrogen, (b) hydrogen enrichment in reverted austenite and (c) hydrogen enrichment around the crack tip induced by the stress concentration.

1. Introduction

Although hydrogen embrittlement (HE) has been widely investigated [1–4], it still affects almost all metals and alloys and causes severe failures. Hydrogen-induced cracking or hydrogen blistering can nucleate at the sites of high hydrogen concentrations. It is of great importance to study the hydrogen distribution for a better understanding of the HE mechanism. Hydrogen microprint technique (HMT) [5,6], second ion mass spectrometry (SIMS) [7,8] and tritium autoradiography [9] have been employed to study the distribution of hydrogen in materials. However, the spatial resolution of these techniques is limited, and the operation is also complex.

The ingress of hydrogen into metals not only degrades the mechanical properties [10–12] but also affects the surface potential or the work function [13–16]. The surface potential here means the contact potential difference (CPD) between the tip of atomic force microscopy (AFM) and the sample [17]. CPD is defined as $V_{CPD} = (\phi_{tip} - \phi_{sample})/e$, where ϕ_{tip} and ϕ_{sample} are the work functions of the tip and the sample, and e is the value of the electronic charge.

The variation of the surface potential that resulted from hydrogen charging was observed by Senöz [18]. With the aid of scanning Kelvin probe force microscopy (SKPFM), hydrogen-induced pitting corrosion in duplex stainless steel was studied [19]. In this study, the continuous evolution of hydrogen dependence behaviour and the enrichment at some sites and the crack tip in maraging steel 18Ni were studied.

2. Materials and methods

The material used in this study was 18Ni maraging steel. The steel was solution treated at 820 °C for 1 h, air cooled and then aged at 510 °C for 3 h. Disk samples with a dimension of Φ 20 mm × 1 mm were machined. The sample surface was mechanically polished. A Vickers mark was made on the surface for *in situ* observation. Previous studies showed that the critical charging current density for the formation of hydrogen blister was 30 mA/cm^2 in 0.2 mol/l NaOH electrolyte with an addition of 0.22 g/l thiourea (H_2NCSNH_2) [20]. Therefore, 5 mA/cm^2, the value of the applied current density during the pre-charging process in the same solution for 24 h should not cause the formation of hydrogen blister or non-reversible hydrogen damage.

The morphology and the surface potential were measured by using an AFM before and after hydrogen charging. The electrochemical pre-charged wedge-open loading sample was employed to investigate the evolution of the surface potential around the crack tip. All the experiments were carried out at room temperature.

3. Results and discussions

The surface topography of uncharged and charged samples was measured by SKPFM, as shown in Fig. 1(a) and (b), respectively. The white profile superimposed in Fig. 1 reveals the height fluctuation of the samples. The surface roughness was measured in 5 randomly selected areas. The average surface roughness was 1.08 nm and 1.64 nm for the uncharged and charged samples, and the corresponding error was 0.03 nm and 0.14 nm, respectively. The surface roughness of

---

* Corresponding author. Tel.: +86 10 62334493; fax: +86 10 62332345.
E-mail address: jxli65@ustb.edu.cn (J. Li).

1388-2481/$ – see front matter © 2013 Elsevier B.V. All rights reserved.
http://dx.doi.org/10.1016/j.elecom.2013.08.006

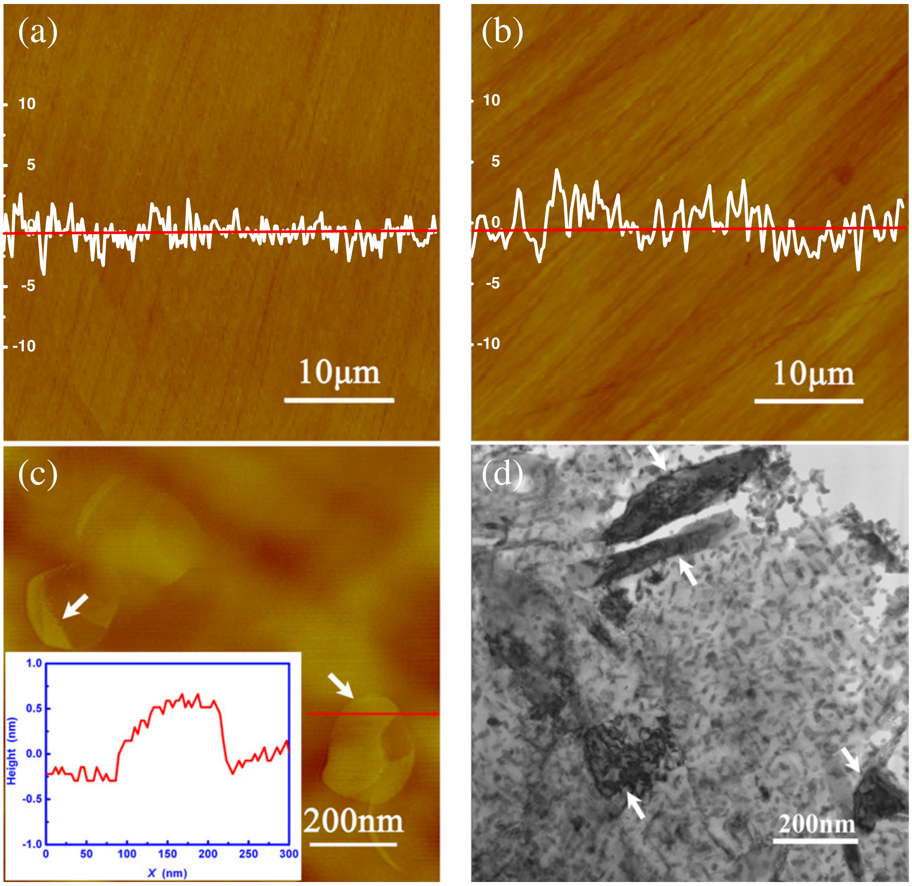

Fig. 1. (a) Surface topography of uncharged and (b) hydrogen charged sample. The insets in (a) and (b) are the profiles of the topography and the unit is nm. (c) Topography of the hydrogen charged sample (more microscopic), and the inset in (c) is the profile of the topography, which marked by a red line. (d) TEM image showing reverted austenite existing in the matrix, pointed by arrows.

uncharged sample was measured immediately after polishment. Afterward, the same sample was subjected to hydrogen tests. Therefore, the difference of the surface roughness was not due to mechanical polishing. The detailed topography of the hydrogen charged sample was shown in Fig. 1(c). There were some bulges marked by the arrows. Most of them were about tens of nanometers, which were 0.5–1.0 nm in height, as shown in the inset. However, the bulges were not observed on the uncharged samples. This means that the difference of the surface roughness was caused by hydrogen.

Fig. 1(d) shows that there are some reverted austenites in the matrix. It was known that dissolved hydrogen in metal can lead to a lattice expansion [21,22]. For example, the lattice constant of 310 austenite stainless steel could increase 2.1% and 5.5% when the hydrogen pressures were 2.3 GPa and 7 GPa [23]. Hydrogen has higher solubility and lower diffusivity in the austenite phase than in martensite, so that the lattice expansion in the austenite phase is larger than in martensite. The dimensions of reverted austenite in Fig. 1(d) matched well with these bulges, so it infers that these bulges were induced by the expansion of reverted austenite.

Fig. 2(a) shows the surface potential of the uncharged sample. It is found that the surface potential distribution is homogeneous and the average value is about 489 mV. After hydrogen charging for 24 h, there are some “white points” in the image, indicating that the surface potentials of these points are higher than the other regions, as shown in Fig. 2(b) and (f). Fig. 2(f) is the 3D SKPFM image of the surface potential after hydrogen charging. Fig. 2(b)–(e) are the continuous evolution of the surface potential images with hydrogen escaping from the same region. One can find that “white points” became weaker and weaker in intensity with time.

More data were obtained to illustrate the time dependence of the work function after hydrogen charging. In Fig. 3, the corresponding data of the dots are taken from the same “white point,” marked by the arrow in Fig. 2(b). And the data of the square are the average work function of each image. As a comparison, the work function of a hydrogen free sample is 4.897 eV, also presented in Fig. 3. The work function decreased to a lower value after hydrogen charging. It remained to be lower than the hydrogen free sample after 24 h aging. This indicates that hydrogen decreases the work function of the material. Due to the hydrogen-enhanced decohesion mechanism, hydrogen can reduce the cohesive bonding strength of atoms. The energy that electrons escape from the atoms decreases, so the work function decreases after hydrogen charging (comparing the dash line and the solid line in Fig. 3).

The work function increased rapidly at the beginning and then became relatively slowly. The value decreased again after some time. The variation of the work function with time corresponds to the behaviour of the hydrogen desorption on the surface. The hydrogen concentration was higher on the surface at the beginning, and then it sharply decreased due to the release of hydrogen at the very near surface. Meanwhile, hydrogen in the inner sample diffused to the surface and resulted in the increase of hydrogen concentration. The hydrogen concentration on the surface would decrease again with the exhaust of the inner hydrogen so that the work function increased also. The concentration near the surface was dynamically controlled by the hydrogen desorption and diffusion processes, and then the work function was changed with the hydrogen concentration. Although the diffusible hydrogen released from the sample, there was still some trapped hydrogen or dissolved hydrogen, which